Applied Catalysis B: Environmental 123–124 (2012) 1–8

Contents lists available at SciVerse ScienceDirect

Applied Catalysis B: Environmental

journal homepage: www.elsevier.com/locate/apcatb

Fast photocatalytic degradation of rhodamine B over $[Mo_6Br_8(N_3)_6]^{2-}$ cluster units under sun light irradiation

Alexandre Barras[a], Stéphane Cordier[b], Rabah Boukherroub[a,*]

[a] Institut de Recherche Interdisciplinaire (IRI, USR CNRS 3078), Université de Lille 1, Parc de la Haute Borne, 50 Avenue de Halley, BP 70478, 59658 Villeneuve d'Ascq, France
[b] Université de Rennes 1, Institut Sciences Chimiques de Rennes, UR1-CNRS 6226, Equipe Chimie du Solide et Matériaux, Campus de Beaulieu, CS 74205, 35042 Rennes Cedex, France

ARTICLE INFO

Article history:
Received 19 November 2011
Received in revised form 30 March 2012
Accepted 4 April 2012
Available online 17 April 2012

Keywords:
$[Mo_6Br_8(N_3)_6]^{2-}$ cluster unit
Rhodamine B
Photodegradation
Sun light

ABSTRACT

The paper reports on the high photocatalytic activity of $[Mo_6Br_8(N_3)_6]^{2-}$ cluster units for the degradation of rhodamine B under UV, visible or sun light irradiation. Water soluble $Na_2[Mo_6Br_8(N_3)_6]$ inorganic compound built up from $[Mo_6Br_8(N_3)_6]^{2-}$ anionic cluster units associated with Na^+ counter cations investigated in this work is prepared in high yield by the interaction of Mo_6Br_{12} with sodium azide in methanol. The high photocatalytic performance of the molybdenum cluster is demonstrated under real solar light excitation, suggesting that the photocatalyst could be used in broad daylight hours. Furthermore, the cluster is still highly active after ten successive cycling runs under UV or visible light irradiation without any apparent loss of its efficiency.

1. Introduction

Dyes are profusely used in multiple applications such as textiles, papers, leathers, additives, food and cosmetics. Due to their large-scale production and chemical stability, dyes can cause considerable environmental pollution [1]. Advanced physicochemical methods such as photocatalysis appear to be a promising technology that has a number of applications in environmental systems such as elimination of hazardous chemical compounds from water and air [2].

Semiconductor materials, including TiO_2, WO_3, Ta_2O_5, ZnS and CdS have been largely used as heterogeneous photocatalysts for the efficient photodegradation of several organic pollutants present in water wastes [2]. Although much work in photocatalysis has focused on TiO_2, its wide bandgap (3.2 eV) requires UV light irradiation. Or only about 4% of the solar spectrum falls in the UV range. This limits the efficient utilization of solar energy for TiO_2 photocatalysis. Another class of photocatalysts, well-defined metal oxide complexes, polyoxometallates (POM), have also been successfully applied for the photocatalytic mineralization of various organic pollutants [3]. However, most of the metal oxides are large band gap semiconductors. Thus, only light below 400 nm is capable of producing electron–hole pairs [3].

Recently, the development of new visible or sun light-driven photocatalysts for pollutant degradation has emerged. Several efforts have been focused to design multiple-metal oxide semiconductors containing molbydates that are efficient for organic molecule decomposition under visible light irradiation, such as Bi_2MoO_6 [4–8], $Bi_2Mo_2O_9$ [9], or $Bi_2Mo_3O_{12}$ [10].

In the search for new photocatalysts, we report in this communication on the high performance of $[Mo_6Br_8(N_3)_6]^{2-}$ cluster units [11,12] for the photodegradation of rhodamine B (RhB). The $Na_2[Mo_6Br_8(N_3)_6]$ cluster precursor is easily prepared via solution chemistry route starting from Mo_6Br_{12} precursor. The photocatalytic activity of the $[Mo_6Br_8(N_3)_6]^{2-}$ cluster unit was evaluated on a model system, rhodamine B, under UV, visible light and direct solar light irradiation. Our results suggest that the $[Mo_6Br_8(N_3)_6]^{2-}$ cluster unit is very efficient even under day light irradiation. Indeed, a full decoloration of an aqueous solution of RhB under exposure to sun light was observed after only 150 min.

2. Experimental

2.1. UV–vis spectrometry

Absorption spectra were recorded using a PerkinElmer Lambda UV–vis 950 spectrophotometer in a spectrometric quartz cuvette with an optical path of 10 mm. The wavelength range was 200–800 nm. The reflectance spectra were recorded using the angle absolute universal reflectance accessory (URA) from PerkinElmer.

* Corresponding author. Tel.: +33 3 62 53 17 24; fax: +33 3 62 53 17 01.
E-mail address: rabah.boukherroub@iri.univ-lille1.fr (R. Boukherroub).

0926-3373/$ – see front matter © 2012 Elsevier B.V. All rights reserved.
http://dx.doi.org/10.1016/j.apcatb.2012.04.006

The cluster was pressed into a pellet under a 10 ton load for 2–4 min. The pellet thickness is about 1 mm.

2.2. Preparation of $Na_2[Mo_6Br_8(N_3)_6]$

500 mg of NaN_3 were introduced in a Schlenk container with 20 mL of methanol at 55 °C. After dissolution of NaN_3, 1 g of $MoBr_2$ was added to the solution. After one night of reaction, a clear solution was obtained. After filtration and evaporation of methanol, $Na_2[Mo_6Br_8(N_3)_6]$ was separated from excess of NaN_3 and NaBr by 3 successive extractions with dry acetone. Yield: 74%. EDS Na: 12; Mo: 41; Br: 47 (theo: 12.5/37.5/50). The presence of N_3 on the cluster was confirmed by IR analysis [12].

2.3. Photodegradation of RhB under UV or visible light irradiation

The catalytic properties of the $Na_2[Mo_6Br_8(N_3)_6]$ cluster have been evaluated for the photocatalytic degradation of RhB in an aqueous solution. The photocatalytic degradation reaction was carried out in a 1 cm spectrometric quartz cuvette containing 2 mL of 10 mg L^{-1} RhB and the photocatalyst at different concentrations: 10, 20, or 30 mg L^{-1}.

For UV light irradiation, the RhB aqueous solution was irradiated without stirring at room temperature in air through with a cut off filter (λ = 365 nm) using a UV fiber lamp (Spot Light Source 300–450 nm, L9588-01, Hamamatsu, Japan). The intensity of the light was measured using a C6080 Series UV Power Meter (Hamamatsu, Japan) and was determined as being 0.5 W cm^{-2}.

For visible light irradiation, the RhB aqueous solution was irradiated without stirring at room temperature in air through with a cut off filter (λ = 420 nm, to suppress the light with wavelength shorter than 420 nm) using a visible fiber lamp (Spot Light Source 400–700 nm, L9566-03, Hamamatsu, Japan). The intensity of the light was measured using a PM600TM Laser Fiber Power Meter (Coherent Inc, USA) and was determined as being 0.5 W cm^{-2}.

The whole quartz cuvette was directly transferred at different irradiation time intervals in a UV–vis spectrophotometer. The concentration of RhB was determined by monitoring the changes in the absorbance maximum at ca. 554 nm.

2.4. Photodegradation of RhB under sun light irradiation

A Pyrex glass vessel containing 20 mL aqueous solution of 10 mg L^{-1} of RhB and photocatalyst at 10 and 30 mg L^{-1}, respectively was exposed to solar radiation in a sunny day for 2 h. The temperature of the system was around 29 °C. In this case, various aliquots (2 mL) were taken at different time intervals and analyzed using UV–vis spectrophotometer.

2.5. HPLC analysis

High performance liquid chromatography (HPLC) analysis was performed on a Shimadzu LC2010-HT (Shimadzu, Tokyo, Japan) using a 5 μm C_4 QS Uptisphere® 300 Å, 250 mm × 4.6 mm column (Interchim, Montluçon, France) heated to 40 °C. The mobile phase was a mixture of eluent A (trifluoroacetic acid 0.05% in H_2O) and eluent B (trifluoroacetic acid 0.05% in CH_3CN) at a flow rate of 1 mL/min. The linear gradient was 0–80% of eluent B in 30 min and the detection was performed at 520 nm. At given intervals during irradiation, the RhB solution was filtered through a Minisart RC filter (pore size 0.2 μm) to remove the photocatalyst and analyzed directly without dilution by injecting 10 μL into the HPLC column.

2.6. MS analysis

LC–ESI–MS analyses were performed on a triple quadrupole mass spectrometer (Quattro II Micromass-Waters) equipped with an electrospray ion source coupled with high pressure liquid chromatography system (HP1100 Agilent). Filtrates were injected (10 μL) on a C18 column (Kromasil 250 mm × 2 mm i.d, 5 μm, Interchim) heated to 30 °C. The flow rate was set at 150 μL min^{-1}. The mobile phase was a mixture of solvent A (0.1% formic acid in H_2O) and solvent B (0.1% formic acid in CH_3CN). The elution gradient was 10–80% of solvent B in 30 min and visible detection was performed at 520 nm. The mass spectrometer was operated in the positive ion mode. The source parameters were the following: spray voltage 3.5 kV, cone voltage 30 V, source temperature 120 °C. Data were acquired in full scan MS mode over the range m/z 220–500.

3. Results and discussion

Metal atom octahedral clusters prepared by solid-state chemistry are nanosized molecular units that exhibit specific physico-chemical properties such as a large absorption window from UV to visible and a large emission window from red to near infrared. Their properties originate from the delocalization of valence electrons on all metal centers [13,14]. The cluster is covalently bonded to eight inner face-capping ligands. It is additionally linked to six more labile apical ligands in terminal position that enable the functionalization of the cluster in solution. After dissolution, they can be used as useful building blocks in the elaboration of molecular assemblies, nanomaterials and functional surfaces by solution chemistry [15–18]. Among all Mo_6 cluster units found in the literature, it turns out that $[Mo_6Br_8(N_3)_6]^{2-}$ units associated with Na^+ cations dissolve in water without immediate precipitation by formation of hexahydroxo complexes. The $[Mo_6Br_8(N_3)_6]^{2-}$ cluster units used in this work were prepared by the interaction of Mo_6Br_{12} solid-state compound with sodium azide in methanol [11,12]. Fig. 1 displays a schematic representation of the $[Mo_6Br_8(N_3)_6]^{2-}$ anionic unit built up from Mo_6 clusters linked to eight face capping bromine atoms and to six apical azide groups.

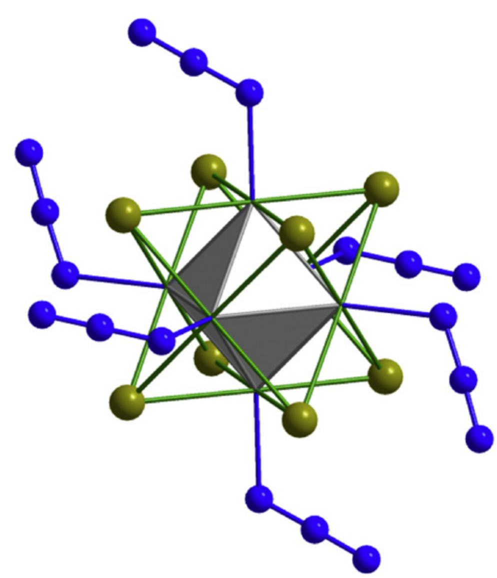

Fig. 1. Representation of the $[Mo_6Br_8(N_3)_6]^{2-}$ anionic unit. The octahedral cluster is represented as a grey octahedron. Bromine and nitrogen atoms are represented as green and blue spheres, respectively. (For interpretation of the references to color in this figure legend, the reader is referred to the web version of the article.)

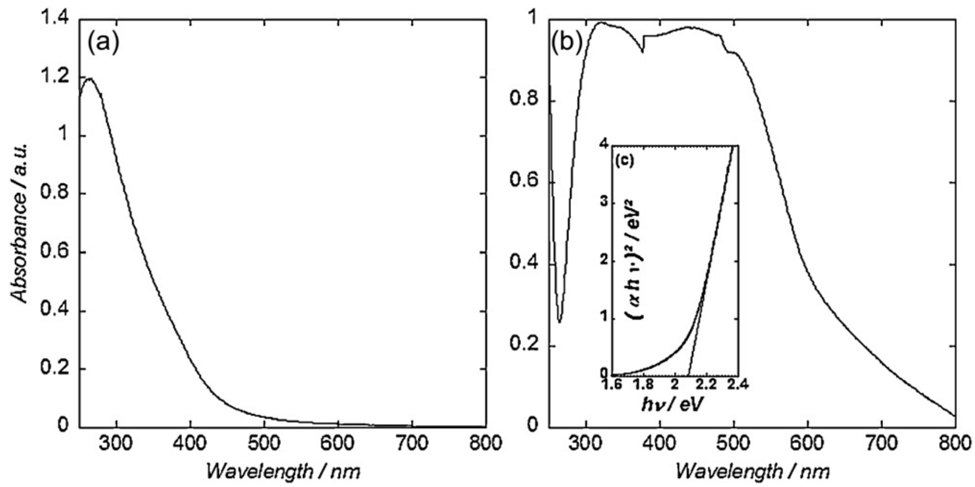

Fig. 2. (a) UV–vis absorption spectrum of $Na_2[Mo_6Br_8(N_3)_6]$ cluster at 30 mg L^{-1} in water; (b) UV–vis reflectance spectrum of $Na_2[Mo_6Br_8(N_3)_6]$ cluster in the solid state; (c) the inset shows the $(\alpha h\nu)^2$ versus $h\nu$ plot.

UV–vis absorption spectrum of $Na_2[Mo_6Br_8(N_3)_6]$ in water (30 $\mu g\,mL^{-1}$) indicates that the photocatalyst absorbs from the UV region to wavelengths shorter than 480 nm with an absorption maximum at around 260 nm (Fig. 2a).

It is well-established that upon irradiation of a semiconductor material, there is a migration of an electron from the valence band to the conduction band, yielding a hole in the valence band. The created electron–hole pair might undergo charge transfer to adsorbed

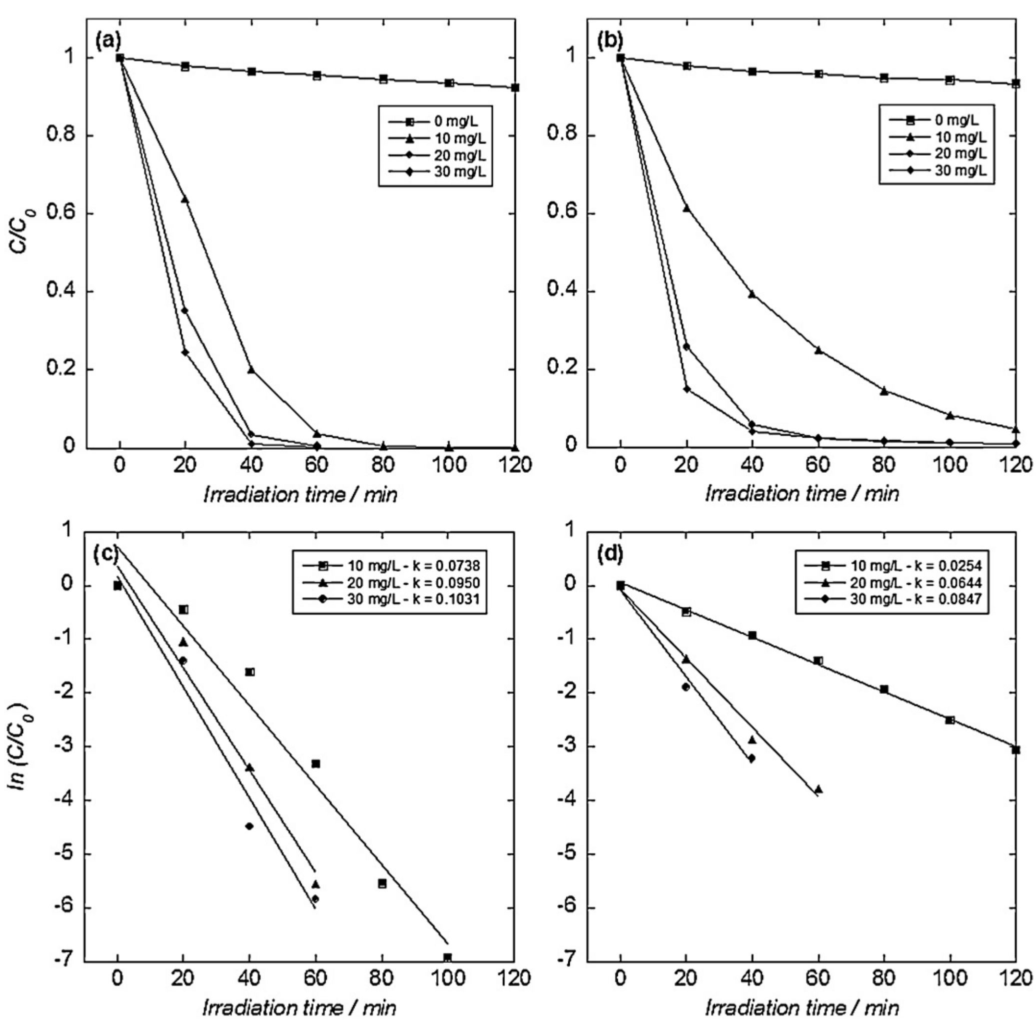

Fig. 3. Temporal course of photocatalytic degradation of rhodamine B at different concentrations of $Na_2Mo_6Br_8(N_3)_6$ cluster precursor under UV (a) and visible light (b) irradiation; $\ln(C/C_0)$ versus irradiation time under UV (c) and visible light (d) irradiation.

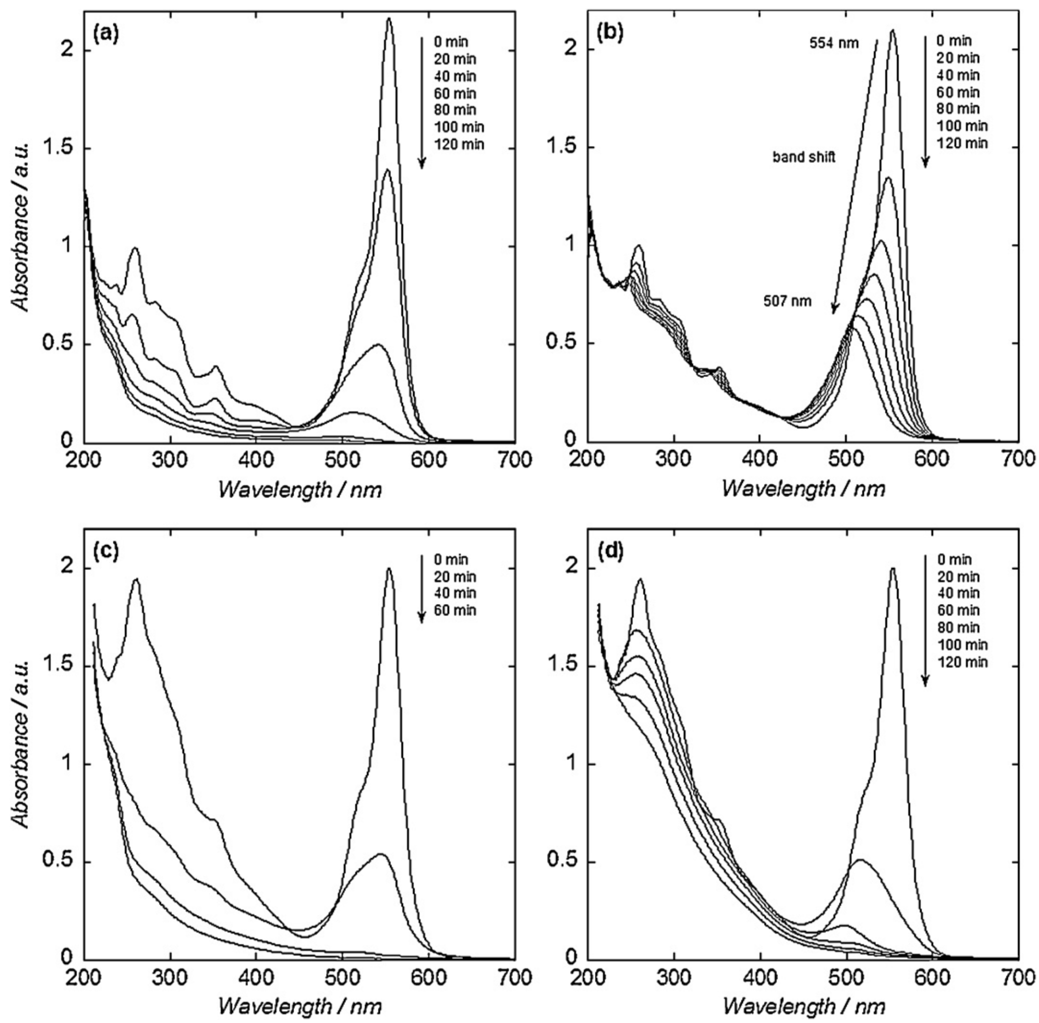

Fig. 4. UV–vis absorption spectra of rhodamine B before and after irradiation in the presence of $Na_2[Mo_6Br_8(N_3)_6]$ cluster precursor at 10 mg L^{-1} (a and b) and at 30 mg mL^{-1} (c and d) as a function of irradiation time under UV light (a–c) and visible light (b–d); The initial concentration of rhodamine B is 10 mg L^{-1}, lamp power = 0.5 W.

species on the semiconductor surface, leading to a photocatalytic process. Thus it is mandatory to know the photoabsorption characteristics of the photocatalyst under investigation. Fig. 2b displays the UV–vis reflectance spectrum of $Na_2[Mo_6Br_8(N_3)_6]$. It shows photoabsorption properties from UV to visible light region below 800 nm, suggesting that the cluster is potentially photoactive under visible light irradiation.

For a semiconductor sample, it is possible to determine the optical absorption near the band edge by the equation $(\alpha h\nu)^2 = A(h\nu - E_g)$, where α is the absorption coefficient, h is the Planck constant, and A is a material related constant, and $h\nu$ is the photon energy [19]. From extrapolation of the plot of $(\alpha h\nu)^2$ versus $h\nu$, also called Tauc plot (Fig. 2c), an E_g value of ~2.08 eV is deduced, indicating that $Na_2[Mo_6Br_8(N_3)_6]$ cluster can absorb visible light. This value is lower than 2.58 eV and 2.79 eV reported for Bi_2MoO_6 and Bi_2WO_6, respectively [7].

RhB, a common dye in the xanthene family, was chosen as the model of organic pollutant to investigate the photocatalytic activity of $[Mo_6Br_8(N_3)_6]^{2-}$ cluster unit. The photocatalytic degradation was carried out at room temperature in a quartz cuvette containing 2 mL of RhB in water with an initial concentration of 10 mg L^{-1} and 0, 10, 20, or 30 mg L^{-1} of photocatalyst. An aqueous solution of RhB displays a strong and characteristic absorption band at 554 nm with a shoulder at 520 nm. The photocatalytic performance was monitored by the decay of the absorption of the dye as a function of irradiation time by UV–vis spectroscopy. The photocatalytic activity of the $[Mo_6Br_8(N_3)_6]^{2-}$ cluster unit are compared under UV light (λ = 365 nm) and visible light (λ > 420 nm). The temporal course of photocatalytic degradation of RhB at different concentrations of $Na_2[Mo_6Br_8(N_3)_6]$ cluster precursor are displayed in Fig. 3. In all cases, the characteristic absorption band of tetraethylated RhB at 554 nm decreases during irradiation time. In a control experiment, direct irradiation of an aqueous solution of RhB (in the absence of photocatalyst) showed less than 10% degradation after 120 min under UV or visible light irradiation under otherwise identical experimental conditions.

The effect of the cluster concentration on the photocatalytic performance was investigated. A variation of the $Na_2[Mo_6Br_8(N_3)_6]$ cluster precursor concentration from 10 to 30 mg L^{-1} showed a significant change of the decomposition rate of RhB (Fig. 3a and b). The variation is more noticeable under visible than UV light irradiation. Indeed, after 60 min irradiation, RhB decolorization is almost complete for the photocatalyst concentrations of 20 and 30 mg L^{-1} while the degree of decolorization is about 75% for a concentration of 10 mg L^{-1}. On the other hand, the photodegradation rate is comparable for cluster concentrations of 20 and 30 mg L^{-1} under both UV and visible light irradiation even though the rate is slightly higher under UV irradiation. A full decomposition of RhB was observed after 40 min under UV irradiation, while it requires about 60 min to achieve similar efficiency under

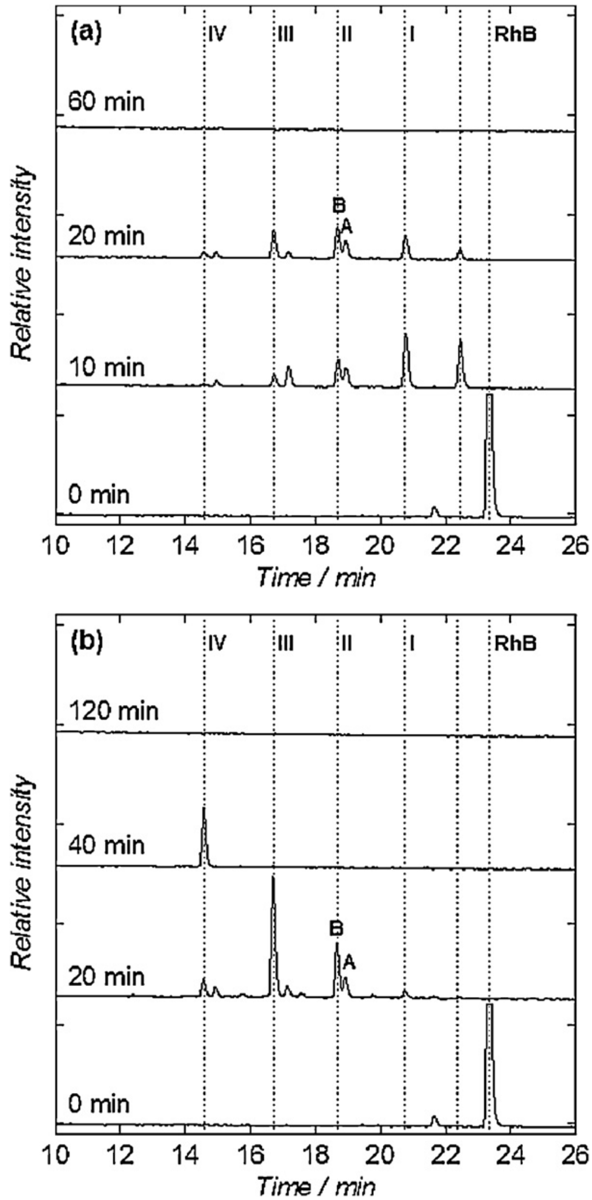

Fig. 5. HPLC chromatograms of the RhB and intermediates recorded at 520 nm after UV (a) and visible light (b) irradiation in the presence of $Na_2[Mo_6Br_8(N_3)_6]$ cluster at 30 mg mL^{-1}; The initial concentration of RhB is 10 mg L^{-1}, lamp power = 0.5 W.

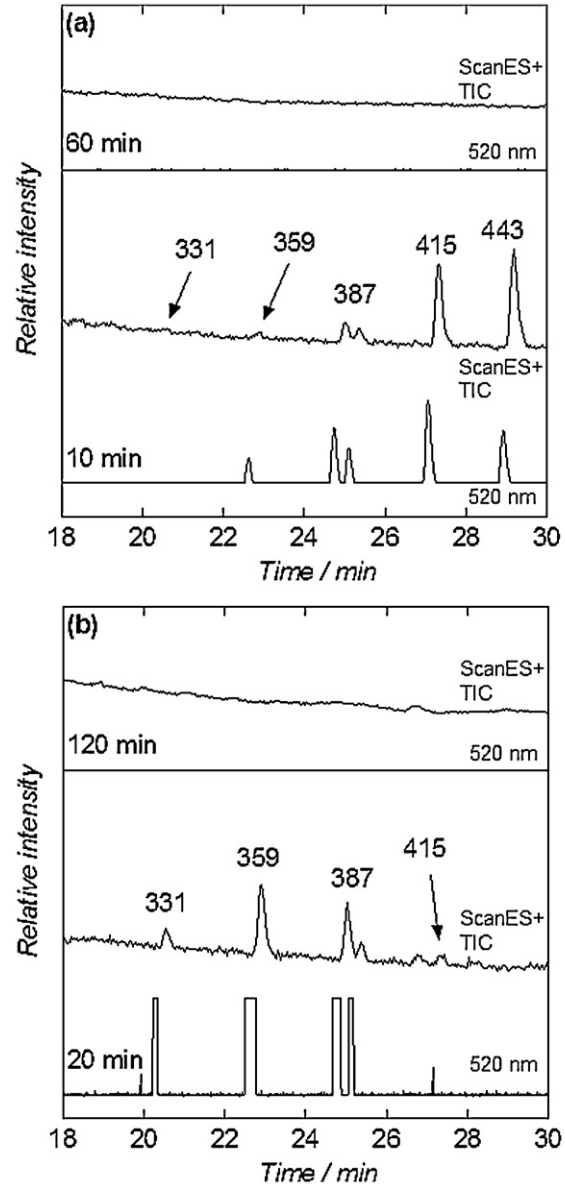

Fig. 6. LCMS and HPLC chromatograms of the RhB and intermediates recorded at 520 nm after UV (a) and visible light (b) irradiation.

visible light irradiation. The photodegradation process follows roughly a pseudo-first-order law by plotting $\ln(C/C_0)$ versus irradiation time (Fig. 3c and d). Kinetic apparent rate constants of 0.074, 0.095 and 0.103 min^{-1} were determined for UV irradiation, while lower apparent rate constants of 0.025, 0.064 and 0.085 min^{-1} were estimated for visible irradiation for $Na_2[Mo_6Br_8(N_3)_6]$ cluster concentrations of 10, 20 and 30 mg L^{-1}, respectively. From these results, it clearly appears that the decomposition rate of the RhB increased from 10 to 30 mg L^{-1}. Further increase of the Mo cluster concentration to 50 mg L^{-1} (data not shown) did not show any increase of the decomposition rate. This observation suggests that the optimal concentration of Mo cluster is around 30 mg L^{-1} and a saturation effect is observed above this concentration.

Fig. 4 exhibits UV/vis spectra of rhodamine B before and after UV ($\lambda = 365$ nm) and visible light ($\lambda > 400$ nm) irradiation in the presence of $Na_2[Mo_6Br_8(N_3)_6]$ cluster precursor at 10 and 30 mg L^{-1}. Under UV irradiation, the characteristic absorption band of RhB at 554 nm decreases significantly with increasing irradiation time without appearance of other absorption features. The decrease of the absorption band at 554 nm is accompanied by a decrease of the absorption at 260 nm due to aromatic fragments. The result suggests that the RhB bleaching occurs mainly via the destruction of the aromatic network (Fig. 4a–c) [20]. Compared to UV irradiation, visible light irradiation of an aqueous solution of RhB shows a decrease of the absorption band at 554 nm accompanied with a concomitant gradual hypsochromic shift (Fig. 4b–d). The blue shift of the absorption band under visible light irradiation is attributed to a stepwise deethylation of RhB; the ethyl groups of tetraethylated RhB are deethylated one by one (corresponding peak of *N*,*N*,*N*′-triethylated rhodamine at 539 nm, *N*,*N*′-diethylated rhodamine at 522 nm, and *N*-ethylated rhodamine at 510 nm) [7,21]. The fully deethylated molecule (completely *N*-deethylated product of RhB) displays a characteristic absorption band at 498 nm after 120, 60 and 40 min of visible irradiation in the presence of 10, 20 and 30 mg L^{-1} of the photocatalyst, respectively. This deethylation process, predominating during the initial illumination period, involves an indirect photocatalysis [22]. Furthermore, the deethylation process

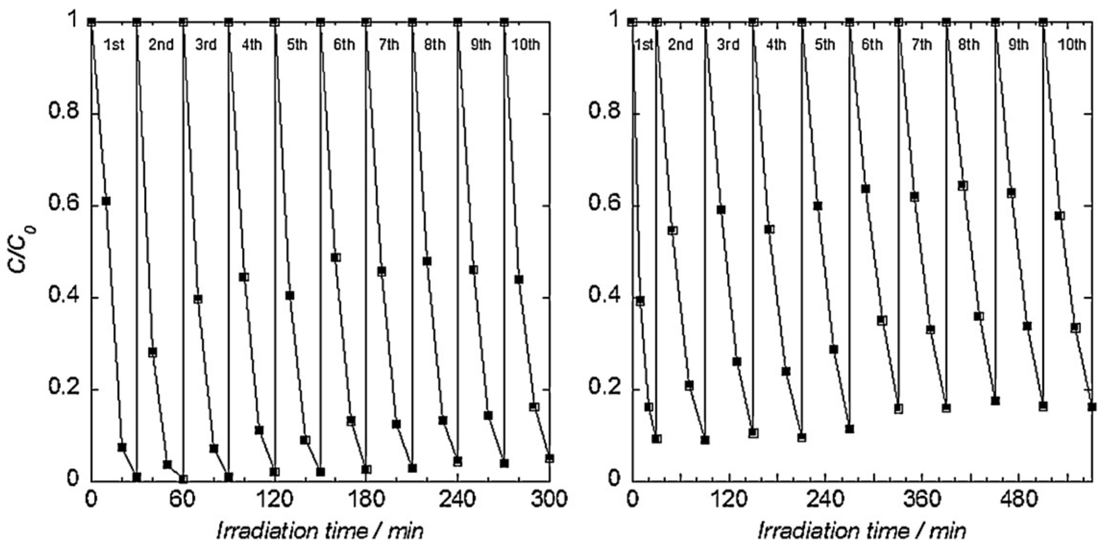

Fig. 7. Cycling experiments in the photocatalytic degradation of rhodamine B in the presence of $Na_2[Mo_6Br_8(N_3)_6]$ cluster precursor at 30 mg L^{-1} under UV (left) and visible light irradiation (right); The initial concentration of rhodamine B is 10 mg L^{-1}, the addition of rhodamine B is 20 μg/run, lamp power = 0.5 W.

facilitates RhB mineralization under visible light irradiation [20]. It is important to note that all absorbance peaks from 498 to 554 nm are reduced during irradiation, indicating that the chromophores of RhB molecules are also degraded.

To confirm the degradation process, the irradiated samples are monitored by HPLC equipped with a UV–vis detector at 520 nm. Temporal variations of HPLC chromatograms under UV or visible light irradiation are exhibited in Fig. 5. RhB aqueous solution with a retention time of 23.3 min is quickly converted into five main intermediates upon UV irradiation. *N*-deethylated intermediates such as *N*,*N*-diethyl-*N*′-ethylrhodamine (I), *N*,*N*-diethylrhodamine (II-A), *N*-ethyl-*N*′-ethylrhodamine (II-B), *N*-ethylrhodamine (III), and rhodamine (IV) with retention times of 20.8, 18.9, 18.7, 16.7, and 14.6 min, respectively are identified based on the reported literature [23,24] (Fig. 5a). Similarly, the intense peak of RhB disappears quickly after 20 min irradiation under visible light, but at the same time the concentration of intermediates increased and subsequently decreased with further irradiation (Fig. 5b). After 60 min of UV and 120 min of visible light irradiation, no intermediate products were detected at 520 nm (and also at 215 and at 254 nm, data not shown), suggesting again the destruction of the conjugated structure of the RhB.

All deethylated intermediates identified by HPLC were further analyzed using LC–MS equipped with an electrospray (ESI) source (Fig. 6). All peaks in the ion chromatograms and corresponding UV–vis chromatograms recorded at 520 nm were separated by 28 *m*/*z* units. Peaks at *m*/*z* 415, 387, 359 and 331 corresponding respectively to intermediate products (I), (II-A and II-B, two isomers), (III) and (IV), from the photodegradation of the initial RhB (*m*/*z* 443), are clearly identified in the MS spectrum.

The activity and stability of $[Mo_6Br_8(N_3)_6]^{2-}$ cluster unit were further investigated by recycling runs. After each run, a fresh concentrated solution of RhB was added to obtain the initial concentration of RhB (10 mg L^{-1}) without causing a significant dilution. Fig. 7 indicates that RhB photobleaching in the presence of the Mo_6 cluster at a concentration of 30 mg L^{-1} takes place in 30 and 60 min under UV and visible light irradiation, respectively after several runs. The cluster is still highly active after ten successive cycling runs under UV or visible light irradiation without any apparent loss of its efficiency.

Finally, the photocatalytic efficiency of the Mo cluster was examined under real conditions i.e. solar light irradiation. A pyrex photoreactor was exposed to solar irradiation in a clear sunny day, taking aliquots at different time intervals. The temporal course of RhB degradation as a function of $Na_2[Mo_6Br_8(N_3)_6]$ concentration is shown in Fig. 8a and b. A quite similar behaviour to that described for visible experiments is observed: a significant increase of the decomposition rate when the cluster concentration is increased from 10 to 30 mg L^{-1}. Here again, an optimal concentration of $Na_2[Mo_6Br_8(N_3)_6]$ is around 30 mg L^{-1}. However, the degradation rate is slower than that obtained using visible light irradiation. Indeed, it requires about 2 h to reach a comparable degree of RhB decolorization using sun light irradiation to that obtained after 40 min using visible light irradiation even though the experimental conditions are not similar (irradiation of 20 mL of RhB under sun light).

The UV–vis absorption spectral changes of RhB under solar irradiation are displayed in Fig. 8c. The characteristic absorption band of RhB at 554 nm decreases considerably upon sunlight exposition. The maximum of absorption shifts to lower wavelengths, according to the deethylation process demonstrated with visible light experiments. Thereby, the photodecomposition process of RhB under direct solar light seems to be dominated by the visible component of the solar energy spectrum. The effective degradation of RhB under solar light excitation is also confirmed by the complete disappearance of the initial pink color of the RhB solution upon irradiation (Fig. 8c).

The mechanistic scheme suggested to take place during the photocatalytic degradation of RhB in the presence of $Na_2[Mo_6Br_8(N_3)_6]$, can be summarized as follows:

$$Na_2[Mo_6Br_8(N_3)_6] \xrightarrow{h\nu} Na_2[Mo_6Br_8(N_3)_6]^*$$
$$\text{i.e. } Na_2[Mo_6Br_8(N_3)_6](h^+ + e^-) \quad (1)$$

$$Na_2[Mo_6Br_8(N_3)_6](h^+ + e^-) + H_2O \rightarrow Na_2[Mo_6Br_8(N_3)_6](e^-) + HO^\bullet + H^+$$
$$HO^\bullet + RhB \rightarrow \text{oxidation products} \rightarrow\rightarrow CO_2 + H_2O + \text{inorganic ions} \quad (2)$$

When the energy $h\nu$ of a photon is equal to or higher than the band gap (E_g) of $Na_2[Mo_6Br_8(N_3)_6]$, there is a generation of an electron–hole pair. Reaction of the photoexcited catalyst with H_2O (i.e. oxidative hole trapping) creates "surface" bound OH radicals (Eqs. (1) and (2)). The hydroxyl radicals react subsequently with RhB in various ways such hydroxylation, H-abstraction, and oxidation products (Eq. (3)).

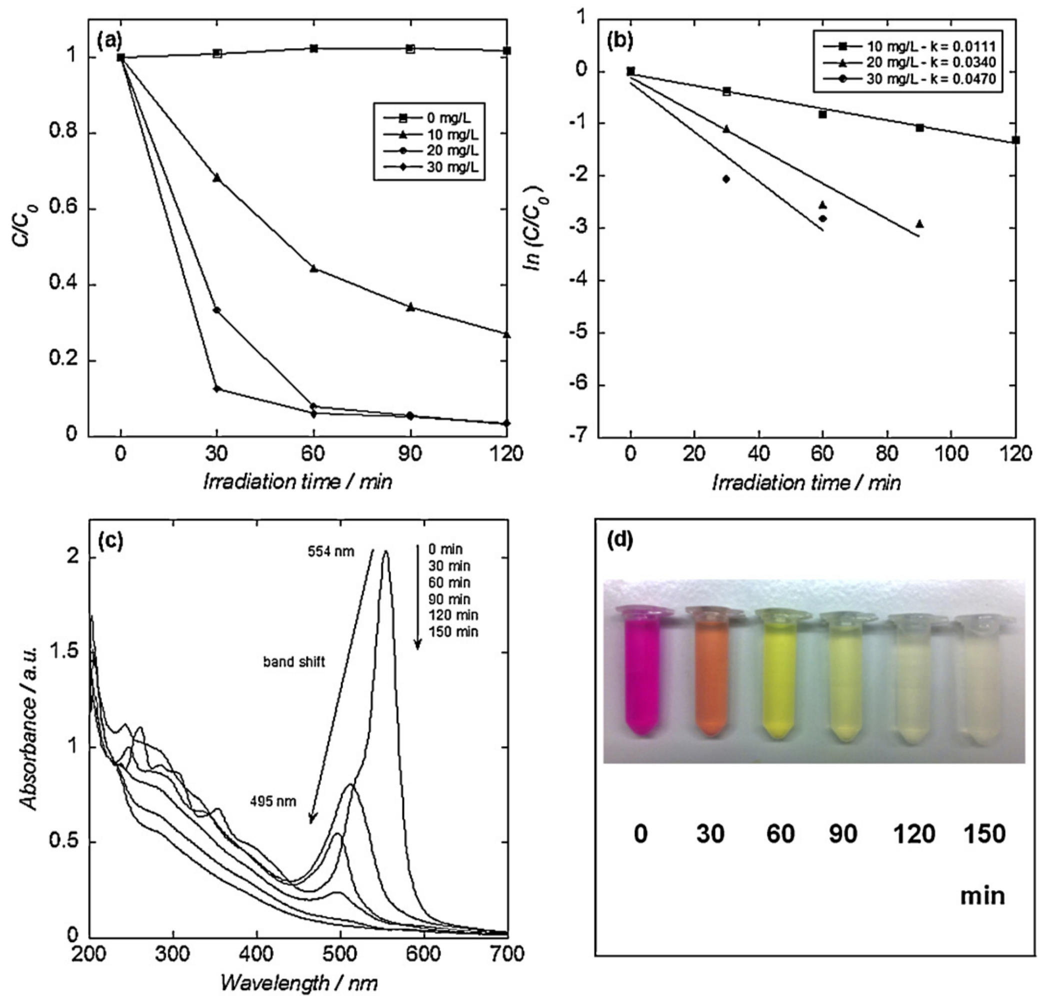

Fig. 8. (a) Temporal course of photocatalytic degradation of RhB at different concentrations of $Na_2[Mo_6Br_8(N_3)_6]$ cluster precursor under direct solar light; (b) first-order re-plot in $\ln(C/C_0)$ versus irradiation time; (c) UV–vis absorption spectra of rhodamine B before and after irradiation in the presence of $Na_2[Mo_6Br_8(N_3)_6]$ cluster precursor at $30\,mg\,L^{-1}$ as a function of irradiation time under direct solar light; (d) photos of RhB solutions before (0) and after solar irradiation for 30, 60, 90, 120, and 150 min in the presence of $Na_2[Mo_6Br_8(N_3)_6]$ cluster precursor at $30\,mg\,L^{-1}$; the initial concentration of RhB is $10\,mg\,L^{-1}$. (For interpretation of the references to color in this figure legend, the reader is referred to the web version of the article.)

Dioxygen is a very effective oxidant for reduced $Na_2[Mo_6Br_8(N_3)_6]$, thus its main action is the regeneration of the catalyst (Eq. (3)). The formation of superoxide radical anion $O_2^{\bullet-}$ ($O_2^{\bullet-} + H^+ \leftrightarrow HO_2^{\bullet}$) may participate further in oxidative as well as reductive processes (Eq. (4)).

$$Na_2[Mo_6Br_8(N_3)_6](e^-) + O_2 \rightarrow Na_2[Mo_6Br_8(N_3)_6](O_2^{\bullet-}) \quad (3)$$

$$\frac{O_2^{\bullet-}}{HO_2^{\bullet}} + S \rightarrow \text{oxidation products} \quad (4)$$

4. Conclusion

In summary, we have demonstrated that the $[Mo_6Br_8(N_3)_6]^{2-}$ cluster unit exhibits excellent photocatalytic performance for the decomposition of RhB under UV and visible light irradiation. A photocatalyst concentration in the range of 20–30 $mg\,L^{-1}$ of the $Na_2[Mo_6Br_8(N_3)_6]$ cluster precursor was found to be optimal for RhB degradation even though the mechanism seems to be wavelength dependent. Furthermore, experiments run under real solar light excitation suggest that the molybdenum cluster could be an efficient catalyst to decompose organic pollutants in broad daylight hours. The results provided in this work hold promise in view of various photocatalytic applications of the Mo_6 cluster under solar light irradiation. An interesting feature is that octahedral clusters can be incorporated in various architectures as for instance porous metal organic frameworks, nanoparticles, polymers or functional surfaces for further heterogeneous photocatalytic studies [25–27].

Acknowledgments

The Centre National de la Recherche Scientifique (CNRS) and the Nord Pas de Calais region are gratefully acknowledged for financial support. The Mass Spectrometry facility used in this study was funded by the European Community (FEDER), the Région Nord-Pas de Calais (France), the CNRS, and the Université Lille 1 Sciences et Technologies.

References

[1] E. Forgacs, T. Cserhati, G. Oros, Environment International 30 (2004) 953.
[2] M.R. Hoffmann, S.T. Martin, W.Y. Choi, D.W. Bahnemann, Chemical Reviews 95 (1995) 69.
[3] A. Hiskia, A. Mylonas, E. Papaconstantinou, Chemical Society Reviews 30 (2001) 62.
[4] J.H. Bi, L. Wu, H. Li, Z.H. Li, X.X. Wang, X.Z. Fu, Acta Materialia 55 (2007) 4699.
[5] A. Martinez-de la Cruz, S.O. Alfaro, E.L. Cuellar, U.O. Mendez, Catalysis Today 129 (2007) 194.

[6] X. Zhao, J.H. Qu, H.J. Liu, C. Hu, Environmental Science and Technology 41 (2007) 6802.
[7] C. Belver, C. Adan, M. Fernandez-Garcia, Catalysis Today 143 (2009) 274.
[8] X. Zhao, T. Xu, W. Yao, Y. Zhu, Applied Surface Science 255 (2009) 8036.
[9] A.M.D. la Cruz, L.G.G. Lozano, Reaction Kinetics Mechanisms and Catalysis 99 (2010) 209.
[10] A. Martinez-de la Cruz, S.O. Alfaro, Solid-State Sciences 11 (2009) 829.
[11] G. Pilet, S. Cordier, S. Golhen, C. Perrin, L. Ouahab, A. Perrin, Solid-State Sciences 5 (2003) 1263.
[12] D. Bublitz, W. Preetz, M.K.Z. Simsek, Zeitschrift für anorganische und allgemeine Chemie 623 (1997) 1.
[13] A.W. Maverick, J.S. Najdzionek, D. MacKenzie, D.G. Nocera, H.B. Gray, Journal of the American Chemical Society 105 (1983) 1878.
[14] J.A. Jackson, C. Turro, M.D. Newsham, D.G. Nocera, Journal of Physical Chemistry 84 (1990) 4500.
[15] S. Cordier, K. Kirakci, D. Méry, C. Perrin, D. Astruc, Inorganica Chimica Acta 359 (2006) 1705.
[16] Y. Molard, F. Dorson, V. Circu, T. Roisnel, F. Artzner, S. Cordier, Angewandte Chemie International Edition 49 (2010) 3351.
[17] S. Ababou-Girard, S. Cordier, B. Fabre, Y. Molard, C. Perrin, ChemPhysChem 8 (2007) 2086.
[18] T. Aubert, F. Grasset, S. Mornet, E. Duguet, O. Cador, S. Cordier, Y. Molard, V. Demange, M. Mortier, H. Haneda, Journal of Colloid and Interface Science 341 (2010) 201.
[19] M.A. Butler, Journal of Applied Physics 48 (1977) 1914.
[20] T.X. Wu, G.M. Liu, J.C. Zhao, H. Hidaka, N. Serpone, Journal of Physical Chemistry B 102 (1998) 5845.
[21] T. Watanabe, T. Takizawa, K. Honda, Journal of Physical Chemistry 81 (1977) 1845.
[22] O. Merka, V. Yarovyi, D.W. Bahnemann, M. Wark, Journal of Physical Chemistry C 115 (2011) 8014.
[23] F. Chen, J. Zhao, H. Hidaka, International Journal of Photoenergy 5 (2003) 209.
[24] K. Yu, S. Yang, H. He, C. Sun, C. Gu, Y. Ju, Journal of Physical Chemistry A 113 (2009) 10024.
[25] D. Dybtsev, C. Serre, B. Schmitz, B. Panella, M. Hirscher, M. Latroche, P.L. Llewellyn, S. Cordier, Y. Molard, M. Haouas, F. Taulelle, G. Ferey, Langmuir 26 (2010) 11283.
[26] M.A. Shestopalov, S. Cordier, O. Hernandez, Y. Molard, C. Perrin, A. Perrin, V.E. Fedorov, Y.V. Mironov, Inorganic Chemistry 48 (2009) 1482.
[27] Y. Molard, F. Dorson, K.A. Brylev, M.A. Shestopalov, Y. Le Gal, S. Cordier, Y.V. Mironov, N. Kitamura, C. Perrin, Chemistry-A European Journal 16 (2010) 5613.